PHYSICAL REVIEW B **89**, 085415 (2014)

Effects of screening on the optical absorption in graphene and in metallic monolayers

Marinko Jablan,[1,*] Marin Soljačić,[2,†] and Hrvoje Buljan[1,‡]
[1]*Department of Physics, University of Zagreb, Bijenička c. 32, 10000 Zagreb, Croatia*
[2]*Department of Physics, Massachusetts Institute of Technology, 77 Massachusetts Avenue, Cambridge, Massachusetts 02139, USA*
(Received 23 October 2013; revised manuscript received 13 January 2014; published 18 February 2014)

Screening is one of the fundamental concepts in solid-state physics. It has a great impact on the electronic properties of graphene, where huge mobilities were observed in spite of the large concentration of charged impurities. While static screening has successfully explained dc mobilities, screening properties can be significantly changed at infrared or optical frequencies. In this paper, we discuss the influence of dynamical screening on the optical absorption of graphene and other two-dimensional electron systems such as metallic monolayers. This research is motivated by recent experimental results that pointed out that graphene plasmon linewidths and optical scattering rates can be much larger than scattering rates determined by dc mobilities. Specifically, we discuss a process in which a photon incident on a graphene plane can excite a plasmon by scattering from an impurity, or a surface optical phonon of the substrate.

DOI: 10.1103/PhysRevB.89.085415 PACS number(s): 73.20.Mf, 73.25.+i

I. INTRODUCTION

In recent years there has been a lot of interest in the field of plasmonics, which seems to be the only viable path toward the realization of nanophotonics, or the control of light at scales substantially smaller than the wavelength [1]. However, plasmonic materials (most notably metals) suffer from large losses in the frequency regimes of interest, which led to a wide search for better materials [2]. A great deal of attention has recently been given to plasmonics in graphene [3,4], which is a single two-dimensional (2D) plane of carbon atoms arranged in a honeycomb lattice [5,6]. One exciting point of interest of 2D materials is that they are tunable. For example, graphene can be doped to high values of electron or hole concentrations by applying gate voltage [5], much like in field effect transistors. Furthermore, graphene can be produced in very clean samples with large mobilities (demonstrated by dc transport measurements) [5,6]. The dc scattering rates would imply small plasmon losses in graphene, however it is still not clear how the scattering rates change with frequency, particularly in the infrared (ir) region. Recent nanoimaging measurements [7] have demonstrated somewhat increased plasmon losses at ir compared to the estimate based on dc transport measurements. Measurements of optical transmission through graphene nanoribbons [8] have demonstrated a strong increase in plasmon linewidth with frequency and losses that are much larger than the dc estimates. However, since the ribbon width in these experiments is very small (10–100 nm), edge scattering can significantly increase the losses. Nevertheless, a similar experiment [9] with graphene nanorings has demonstrated plasmon linewidths that approximately agree with the dc estimate.

Finally, electron energy loss spectroscopy (EELS) [10] on graphene sheets has demonstrated huge plasmon linewidths that increase linearly with plasmon momentum; however, the (dc) transport measurements were not reported, so it is not clear what was the actual quality of the graphene films. It is also interesting to note that similar results [11] were obtained with EELS on monatomic silver film, which could imply a common origin of plasmon damping in these two 2D systems. On the one hand, metallic monolayers might be even more interesting from the point of view of plasmonics since they have an abundance of free electrons even in the intrinsic case, while graphene has to be doped with electrons since it is a zero-band-gap semiconductor. On the other hand, graphene has superior mechanical properties and was demonstrated in a free-standing (suspended) sample while metallic monolayers have only been observed on a substrate.

Instead of calculating plasmon linewidth, we will focus on a directly related problem of optical absorption, which is easier to analyze. In that respect, it was shown experimentally [12] that suspended graphene absorbs around 2.3% of normal incident light in a broad range of frequencies. However, if graphene is doped with electrons, then the Pauli principle blocks some of these transitions and there should be a sudden decrease of absorption below a certain threshold, which should theoretically occur at twice the Fermi energy. Nevertheless, optical spectroscopy experiments [13] have shown that there is still a great deal of absorption even below this threshold. This absorption is much larger than the estimate based on dc measurements. A great deal of theoretical work addressed this problem [14–18], but to our knowledge the experimental results have quantitatively not been explained yet.

In this paper, we focus on optical absorption mediated by charged impurity scattering. As we have already stated, the motivation for studying this problem follows from the fact that typical graphene samples can have large mobilities ($\mu \approx 10\,000$ cm^2/V s) in spite of a huge concentration of charged impurities [19] ($n_i \approx 10^{12}$ cm^{-2}), which is actually comparable to the typical concentration of electrons. The reason one can have such a large mobility is screening [19]. In fact, if one assumes that electrons scatter from bare charged impurities described with the Coulomb potential V_q, then the resulting mobility is almost two orders of magnitude lower than the measured value [19]. The only way to reconcile the experiment and theory is to say that the actual scattering potential is screened to $V_q/\varepsilon(q)$, where $\varepsilon(q)$ is the static

*mjablan@phy.hr
†soljacic@mit.edu
‡hbuljan@phy.hr

dielectric function. However, in the dynamical case, at finite frequency, screening is not so effective and $\varepsilon(q)$ should be replaced with the dynamic dielectric function $\varepsilon(q,\omega)$. This will certainly influence the single-particle excitations where an incident photon excites an electron hole pair through impurity scattering. Moreover, at finite frequency one can have $\varepsilon(q,\omega)=0$ (at the plasmon dispersion) so there exists an additional decay channel where an incident photon excites a plasmon of the same energy, through impurity scattering. In other words, impurities break the translational symmetry (momentum does not need to be conserved), which allows the photon to couple directly to a plasmon mode. Very recently, another group also calculated this process in graphene, but only in the small frequency limit [20]. Here we give the result for the arbitrary frequency (both for metallic monolayers and graphene), which can be very different from the small frequency limit.

More specifically, we calculate the optical absorption in 2D electron systems with randomly arranged charged impurities. First, we discuss the case of metallic monolayers which have a parabolic electron dispersion, and then the case of graphene with Dirac electron dispersion. We focus on a decay channel where the incident photon emits a plasmon through impurity scattering, but we also discuss a case in which the incident photon emits the plasmon and a surface optical phonon of the substrate. For graphene on a SiO_2 substrate, the resulting optical absorption is very small compared to the experimental results [13], and it is not enough to reconcile the difference between theory [14–18] and experiment [13]. On the other hand, we predict large optical absorption by plasmon emission via impurity scattering in suspended graphene. Thus we believe that these ideas can be tested in suspended graphene. Finally, we note that for suspended graphene (metallic monolayers), the small frequency limit [20] gives an order of magnitude lower (larger) result than the more exact RPA calculation.

II. METALLIC MONOLAYERS

The case of the optical absorption in a bulk 3D system with parabolic electron dispersion and randomly arranged impurities was already studied by Hopfield [21]. It is straightforward to extend his result to a 2D system, and here we provide only a brief description of the calculation.

We study a system described by the Hamiltonian $H=H_0+H_{e\text{-}e}+H_l+H_i$, where H_0 represents the kinetic energy of free electrons, $H_{e\text{-}e}$ describes the electron-electron interaction, which is conveniently represented through the screening effect, H_l describes scattering with light, and H_i represents scattering with impurities. Electrons in a metallic monolayer can be described with a parabolic dispersion: $H_0=\mathbf{p}^2/2m^*$, where $\mathbf{p}$ is the electron momentum and m^* is the effective mass of the electron. Next, let us introduce a monochromatic light beam of frequency ω which is described by the electric field $\mathbf{E}(t)=\mathbf{E}_0e^{-i\omega t}+\text{c.c.}$ This wave is incident normally on a 2D electron gas, that is, $\mathbf{E}(t)$ is in the plane of the gas. If we are only interested in a linear response with respect to this electric field, then interaction of electrons with light takes a particularly simple expression: $H_l=-i\frac{e}{m^*\omega}\mathbf{p}\cdot\mathbf{E}_0e^{-i\omega t}+\text{c.c.}$, where we have introduced electron charge $(-e)$. Later on, since momentum is a good quantum number even in an interacting electron system, light scattering (H_l) will not change the many-body eigenstates of $H_0+H_{e\text{-}e}$, but only the eigenvalues; see Ref. [21]. Then, one only needs to do the perturbation theory in the impurity scattering. Unfortunately, this trick (due to Hopfield) works only in systems with parabolic electron dispersion, while in the case of Dirac electrons, such as those found in graphene, one needs to apply the perturbation theory both in light scattering and in impurity scattering, which is a much more tedious task.

We can write the Hamiltonian for impurity scattering as a Fourier sum over wave vectors $\mathbf{q}$: $H_i=\frac{1}{\Omega}\sum_{\mathbf{q}}V_i(q)e^{i\mathbf{q}\cdot\mathbf{r}}$, where Ω is the total area of our 2D system. By calculating the induced current to second order in $V_i(\mathbf{q})$, one can find the real part of the conductivity [21]:

$$\mathrm{Re}\sigma(\omega)=-\frac{e^2}{m^{*2}\omega^3}\frac{1}{\Omega}\sum_{\mathbf{q}}q_x^2\frac{1}{\Omega}|V_i(q)|^2\frac{1}{V_c(q)}\mathrm{Im}\frac{1}{\varepsilon(q,\omega)}. \tag{1}$$

Note that this quantity $[\mathrm{Re}\sigma(\omega)]$ determines the optical absorption in our system. Here $\varepsilon(q,\omega)$ stands for a dielectric function of the electron gas, and $V_c(\mathbf{q})=\frac{e^2}{2\bar{\varepsilon}_r\varepsilon_0 q}$ is the Fourier transform of the Coulomb potential between two electrons in a 2D layer embedded between two dielectrics of average relative permittivity, $\bar{\varepsilon}_r=(\varepsilon_{r1}+\varepsilon_{r2})/2$. We have assumed without loss of generality that the external field points in the x direction ($\mathbf{E}_0=\hat{\mathbf{x}}E_0$) and is parallel to the plane of our 2D electron gas.

In the case of randomly assembled impurities at positions $\mathbf{R}_j$, one can write for the scattering potential $V_i(\mathbf{q})=-V_c(\mathbf{q})\sum_j e^{-i\mathbf{q}\cdot\mathbf{R}_j}$. Note that we are assuming positively charged (e) impurities embedded in a see of negative electrons ($-e$). Then by averaging over random impurity positions, one has $\langle|V_i(\mathbf{q})|^2\rangle=N_iV_c^2(\mathbf{q})$, where N_i is the number of impurities [22].

Equation (1) depends on the loss function $\mathrm{Im}\frac{1}{\varepsilon(q,\omega)}$, which generally contains contribution from single-particle excitations and collective (plasmon) excitations. In this paper, we focus solely on the plasmon contribution, in which case one can write [23]

$$\mathrm{Im}\frac{1}{\varepsilon(q,\omega)}=\frac{-\pi}{\frac{\partial\varepsilon}{\partial\omega}}\delta(\omega-\omega_q), \tag{2}$$

where ω_q is the plasmon frequency determined by the zero of the dielectric function: $\varepsilon(q,\omega_q)=0$. This term then represents the process in which an incident photon excites plasmon of the same energy through impurity scattering.

The δ function from Eq. (2) extracts only a single wave vector from the sum in Eq. (1), which corresponds to the plasmon wave vector at the given frequency ω. Then one is left with integration over the angle $\varphi_{\mathbf{q}}$, which is straightforward to perform since $\int_0^{2\pi}d\varphi_{\mathbf{q}}\cdot q_x^2=\pi q^2$.

Finally, we plot the conductivity from expression (1) in Fig. 1 by using the dielectric function $\varepsilon(q,\omega)$ within the random phase approximation (RPA) given in Ref. [24]. To represent the experiment [11], which studied a silver monolayer on a silicon substrate, we choose $\varepsilon_{r1}=\varepsilon_{\mathrm{Si}}=12$, $\varepsilon_{r2}=1$, the effective mass $m^*=0.3m$, where m is the free-electron mass, electron concentration $n=2\times10^{13}\ \mathrm{cm}^{-2}$, and we assume the impurity concentration $n_i=10^{12}\ \mathrm{cm}^{-2}$.

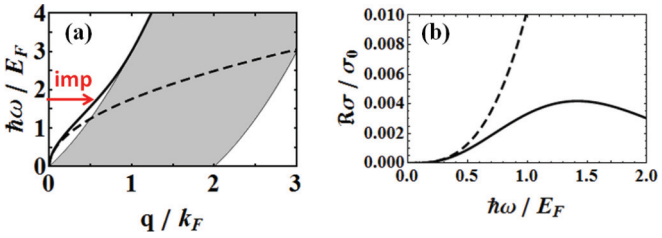

FIG. 1. (Color online) Plasmon dispersion and optical conductivity for metallic monolayers. In plot (a) we show the plasmon dispersion relation within the random phase approximation (solid line) and within the Drude model, i.e., in the small frequency limit (dashed line). The gray area denotes the regime of single-particle excitations. Random assembly of impurities breaks the translation invariance, which allows a zero-momentum photon to couple to a finite-momentum plasmon (sketched by the red arrow). In plot (b) we show the optical absorption for the plasmon emission process through impurity scattering. We plot the real part of the conductivity in units of $\sigma_0 = \frac{e^2}{4\hbar}$ vs photon energy in units of Fermi energy E_F. One can see that the small frequency limit (dashed line) significantly overestimates the more exact RPA result (solid line).

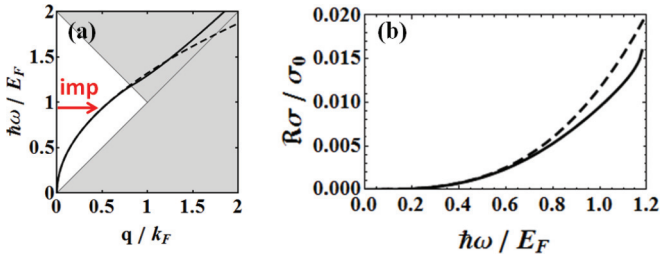

FIG. 2. (Color online) Plasmon dispersion and optical conductivity for graphene sitting on the SiO_2 substrate with air above. In plot (a) we show plasmon dispersion within the random phase approximation (solid line) and within the Drude model, i.e., in the small frequency limit (dashed line). The gray area denotes the regime of single-particle excitations. Random assembly of impurities breaks the translation invariance, which allows a zero-momentum photon to couple to a finite-momentum plasmon (sketched by the red arrow). This process is possible only when the plasmon dispersion is outside of the gray area. Otherwise, plasmons are strongly damped due to single-particle excitations (Landau damping). In plot (b) we show optical absorption for the plasmon emission process through impurity scattering. We plot the real part of the conductivity in units of $\sigma_0 = \frac{e^2}{4\hbar}$ vs photon energy in units of Fermi energy E_F. One can see that the small frequency limit (dashed line) is very close to the more exact RPA result (solid line). This is related to the fact that in this case the plasmon dispersion from (a) is very well described by the small frequency limit.

It is also convenient to look at the small frequency limit ($\hbar\omega \ll E_F$), in which case only long-wavelength ($q \ll q_F$) plasmons contribute to the scattering. Here E_F and q_F stand for Fermi energy and Fermi momentum, respectively. In this limit, one can use a simple Drude model to obtain the dielectric function:

$$\varepsilon_D(q,\omega) = 1 - \frac{q}{\omega^2}\frac{e^2 n}{2\bar{\varepsilon}_r \varepsilon_0 m^*}. \tag{3}$$

In this case, plasmon dispersion is simply $\omega \propto \sqrt{q}$ and one can easily evaluate Eqs. (1) and (2) to obtain the conductivity,

$$\mathrm{Re}\sigma(\omega) = \frac{\pi e^2}{4\hbar}\frac{n_i}{q_{\mathrm{TF}}^2}\left(\frac{\hbar\omega}{E_F}\right)^3. \tag{4}$$

Here we have introduced the Thomas-Fermi wave vector: $q_{\mathrm{TF}} = \frac{e^2 m^*}{2\pi\bar{\varepsilon}_r\varepsilon_0\hbar^2}$, while $n_i = N_i/\Omega$ stands for the impurity density. From Fig. 1(b) we see that in the case of metallic monolayers, the small frequency limit (dashed line) significantly overestimates the more exact RPA result (solid line).

III. GRAPHENE

Unfortunately, the trick that Hopfield used in the case of parabolic dispersion does not work for Dirac dispersion, so one has to apply the perturbation theory both in impurity scattering and light scattering while including the screening effect in every order of the perturbation theory. This is a straightforward but very tedious task, so we give the derivation of the optical absorption in the Appendix. Here we only write the final result:

$$\mathrm{Re}\sigma(\omega) = -\frac{e^2 v_F^2}{\omega}\frac{1}{\Omega}\sum_{\mathbf{q}}\frac{1}{\Omega}\left|\frac{V_i(q)}{\varepsilon(q)}\right|^2 F^2(q,\omega)V_c(q)\mathrm{Im}\frac{1}{\varepsilon(q,\omega)}, \tag{5}$$

where we have assumed a general impurity scattering Hamiltonian: $H_i = \frac{1}{\Omega}\sum_{\mathbf{q}} V_i(q)e^{i\mathbf{q}\cdot\mathbf{r}}$ (see the Appendix for more details). In the case of charged impurities, one has $\langle|V_i(\mathbf{q})|^2\rangle = N_i V_c^2(\mathbf{q})$ after averaging over random impurity positions. Then, to find the contribution of the plasmon emission process, one can use Eq. (2) and the dielectric function which is calculated in Ref. [25] within the RPA. The resulting optical absorption is plotted in Fig. 2. To resemble parameters from the experiment [13], we choose electron concentration $n = 7\times10^{12}$ cm^{-2} and impurity concentration $n_i = 10^{12}$ cm^{-2}. Furthermore, we plot the case of graphene sitting on the SiO_2 substrate where $\bar{\varepsilon}_r = 2.5$, but also the case of suspended graphene where $\bar{\varepsilon}_r = 1$.

It is also convenient to look at the small frequency limit ($\hbar\omega \ll E_F$), in which case only long-wavelength ($q \ll q_F$) plasmons contribute to the scattering. Then, one can use a simple Drude model to obtain the dielectric function in graphene [3]:

$$\varepsilon_D(q,\omega) = 1 - \frac{q}{\omega^2}\frac{e^2 v_F\sqrt{n}}{2\bar{\varepsilon}_r\varepsilon_0\hbar\sqrt{\pi}}. \tag{6}$$

In this case, the function F takes a particularly simple expression (see the Appendix for more details): $F(q,\omega) = \frac{-q_x}{\pi\hbar^2\omega v_F}$, and it is straightforward to evaluate expression (5) to obtain

$$\mathrm{Re}\sigma(\omega) = \frac{\pi e^2}{4\hbar}\frac{n_i}{q_{\mathrm{TF}}^2}\left(\frac{\hbar\omega}{E_F}\right)^3. \tag{7}$$

Note that this is the same result as in the case of metallic monolayers. This is expected because in the small frequency (long-wavelength) limit, one does not expect to see specific details of the band structure. Of course, in the graphene case, the Thomas-Fermi wave vector is given by a different expression: $q_{\mathrm{TF}} = \frac{e^2 q_F}{\pi\bar{\varepsilon}_r\varepsilon_0\hbar v_F}$. We would like to note that the small frequency limit in the case of graphene was also recently

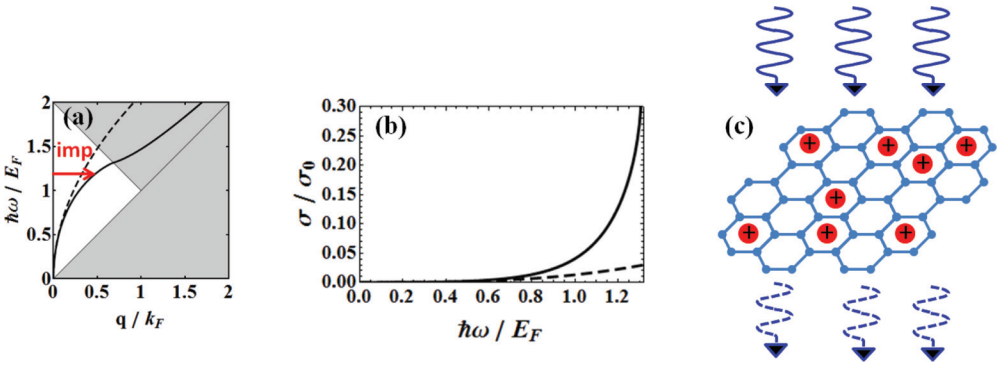

FIG. 3. (Color online) Plasmon dispersion and optical conductivity for suspended graphene. In plot (a) we show plasmon dispersion within the random phase approximation (solid line) and within the Drude model, i.e., in the small frequency limit (dashed line). The gray area denotes the regime of single-particle excitations. Random assembly of impurities breaks the translation invariance, which allows a zero-momentum photon to couple to a finite-momentum plasmon (sketched by the red arrow). This process is possible only when the plasmon dispersion is outside of the gray area. Otherwise, plasmons are strongly damped due to single-particle excitations (Landau damping). In plot (b) we show optical absorption for the plasmon emission process through impurity scattering. We plot the real part of the conductivity in units of $\sigma_0 = \frac{e^2}{4\hbar}$ vs photon energy in units of Fermi energy E_F. One can see that the small frequency limit (dashed line) can be an order of magnitude lower that the more exact RPA result (solid line). The predicted loss mechanism should be observable in optical transmission measurements on suspended graphene, as sketched in plot (c). Red circles with crosses represent positively charged impurity ions that have donated electrons to the graphene plane. See text for details.

obtained by another group [20]. However, from Fig. 3 one can see that the small frequency limit can be very different from the more general RPA result.

If we now compare our results [Fig. 2(b)] with experiment [13], we see that this effect of plasmon emission is relatively small ($\mathrm{Re}\sigma < 0.02\sigma_0$) compared to the experimental results ($\mathrm{Re}\sigma \approx 0.3\sigma_0$) in this regime. One might ask, what are the other potentially strong scattering mechanisms? For example, in experiment [13], graphene is sitting on SiO_2, which is a polar substrate, so there is a strong interaction of electrons with the surface polar phonons at energy $\hbar\omega_{\mathrm{SO}} \approx 0.15$ eV. This is described by the Hamiltonian $H_{\mathrm{SO}} = \frac{1}{\Omega}\sum_{\mathbf{q}} V_{\mathrm{SO}}(q)(e^{i\mathbf{q}\cdot\mathbf{r}}a^{\dagger}_{\mathbf{q}} + e^{-i\mathbf{q}\cdot\mathbf{r}}a_{\mathbf{q}})$, where $a^{\dagger}_{\mathbf{q}}$ is the phonon creation operator. For the square of the scattering potential, we can write [26] $V^2_{\mathrm{SO}}(q) = \Omega\frac{e^2}{2\varepsilon_0}\hbar\omega_{\mathrm{SO}}(\frac{1}{\varepsilon_r(\infty)+1} - \frac{1}{\varepsilon_r(0)+1})\frac{e^{-2qz}}{q}$. We use parameters from Ref. [28] for SO scattering: $\varepsilon_r(0) = 3.9$, $\varepsilon_r(\infty) = 2.5$, and we assume that the Van der Waals distance between graphene and the substrate is $z = 0.35$ nm. If we neglect the frequency dependence of H_{SO}, we can make an estimate of absorption simply by replacing $V_i(q)$ with $V_{\mathrm{SO}}(q)$ in relation (5). Strictly speaking, this is valid only at large frequencies when $\omega \gg \omega_{\mathrm{SO}}$, but it should give a reasonable estimate in the regime $\omega \approx 2\omega_{\mathrm{SO}}$, which is the relevant regime in experiment [13]. The resulting absorption is still extremely small ($\mathrm{Re}\sigma < 0.003\sigma_0$) in the regime of interest ($\hbar\omega \approx E_F$).

Even though our analysis suggests that these loss mechanisms cannot be distinguished from other loss mechanisms in current experiments involving graphene on a SiO_2 substrate, our calculations point out that they should be observable in suspended graphene (see Fig. 3). Suspended graphene is a much cleaner system as one can eliminate all the scattering mechanisms that originate from the interaction with the substrate. Moreover, in optical transmission measurements on suspended graphene [sketched in Fig. 3(c)] one does not need to consider optical absorption of the substrate. Suspended graphene can be doped by depositing electron-donor atoms such as sodium or lithium. In that case, one is left with impurity ions with the same number as the number of injected electrons. In Fig. 3(b) we plot optical absorption in suspended graphene for identical impurity and electron concentrations $n_i = n = 10^{12}$ cm^{-2}. One can see that there is a huge optical absorption through the plasmon emission channel as the real part of conductivity reaches $\mathrm{Re}\sigma \approx 0.3\sigma_0$. This would correspond to the 0.7% reduction in the intensity of transmitted light, which could easily be observed as the 2.3% reduction is already visible with the naked eye [12]. Finally, we note that the small frequency limit [Eq. (7)] underestimates the more exact RPA calculation [Eq. (5)] by an order of magnitude.

IV. CONCLUSION

In conclusion, we have studied the optical absorption of 2D electron gas in graphene and metallic monolayers with a random distribution of charge impurities. This formalism can also treat other 2D electron systems such as those found in heterostructures, single-layer boron nitride, or single-layer molybdenum disulfide, where we expect similar behavior. Specifically, we have focused on a decay channel where an incident photon excites a plasmon through impurity scattering. For the graphene sitting on a SiO_2 substrate, we have also studied a decay channel where an incident photon excites a plasmon and an optical phonon of the polar substrate. The resulting optical absorption is more than one order of magnitude lower than the experimental results [13], which is not enough to reconcile the difference between theory [14–18] and experiment [13]. On the other hand, we predict large optical absorption by plasmon emission via impurity scattering in suspended graphene. Thus we believe that these ideas can be tested in suspended graphene. Finally, we note that for suspended graphene (metallic monolayers), the small frequency limit [20] gives an order of magnitude lower (larger) result than the more exact RPA calculation.

ACKNOWLEDGMENTS

This work was supported in part by the Unity through Knowledge Fund (UKF Grant No. 5/13). The work of M.S. was supported in part by the MIT S3TEC Energy Research Frontier Center of the Department of Energy under Grant No. DE-SC0001299. This work was also supported in part by the Army Research Office through the Institute for Soldier Nanotechnologies under Contract No. W911NF-13-D-0001.

APPENDIX: CALCULATION OF OPTICAL ABSORPTION IN GRAPHENE

We use the single-particle density matrix (SPDM) approach, which is a convenient way to take into account both temperature and the Pauli principle. The equation of motion for SPDM ρ is given by [27]

$$i\hbar\frac{\partial\rho}{\partial t} = [H,\rho], \tag{A1}$$

where the Hamiltonian is given by

$$H = H_0 + H_l + H_i + H^s. \tag{A2}$$

Here H_0 represents the kinetic energy of free electrons, H_l describes scattering with light, H_i represents scattering with impurities, and H^s describes electron-electron interactions, which we only take in the form of a self-consistent screening field. In the case of graphene, electrons are described by Dirac dispersion [28,29]:

$$H_0 = \hbar v_F \boldsymbol{\sigma}\cdot\mathbf{k}, \tag{A3}$$

where $v_F = 10^6$ m/s is the Fermi velocity, $\mathbf{k}$ is the electron wave vector, $\boldsymbol{\sigma} = \sigma_x\hat{\mathbf{x}} + \sigma_y\hat{\mathbf{y}}$, and $\sigma_{x,y}$ are the Pauli spin matrices. Let us denote by $|n\mathbf{k}\rangle$ eigenstates of H_0, where $n = 1$ stands for the conduction band, and $n = -1$ for the valence band. Then the eigenvalues of H_0 are given by Dirac cones: $E_{n\mathbf{k}} = n\hbar v_F|\mathbf{k}|$. If we now introduce a light source described by the electric field $\mathbf{E}(t) = \hat{\mathbf{x}}E_0e^{-i\omega t} + \text{c.c.}$, then scattering with light is determined by the Hamiltonian

$$H_l = -i\frac{ev_F}{\omega}\sigma_x E_0 e^{-i\omega t} + \text{c.c.}, \tag{A4}$$

where $-e$ is the electron charge. Furthermore, we can write the Hamiltonian for impurity scattering as a Fourier sum over wave vectors $\mathbf{q}$:

$$H_i = \frac{1}{\Omega}\sum_{\mathbf{q}} V_i(q)e^{i\mathbf{q}\cdot\mathbf{r}}, \tag{A5}$$

where Ω is the total area of our graphene flake, $\mathbf{r}$ is the position operator, and $V_i(q)$ is the Fourier transform of the scattering potential. Here we assume a general scattering potential, and only later will we specify $V_i(q)$ for the case of charged impurity scattering and surface polar phonon scattering. Finally, one can also write the screening field as a Fourier sum:

$$H^s = \frac{1}{\Omega}\sum_{\mathbf{q}} V^s(\mathbf{q})e^{i\mathbf{q}\cdot\mathbf{r}}e^{-i\omega t} + \text{c.c.}, \tag{A6}$$

but one has to keep in mind that different orders of the perturbation expansion will have a different time dependence (frequencies). Here, the screening field is taken as a self-consistent electrostatic field that the electrons induce on themselves, so one can write $V^s(\mathbf{q}) = V_c(q)n(\mathbf{q})$, where $n(\mathbf{q})$ is the Fourier transform of the electron density and $V_c(q)$ is the Fourier transform of the Coulomb potential between two electrons. For a 2D electron gas embedded between two dielectrics of relative permittivity, $\bar{\varepsilon}_r = (\varepsilon_{r1} + \varepsilon_{r2})/2$, one can write $V_c(q) = \frac{e^2}{2\bar{\varepsilon}_r\varepsilon_0 q}$. Note that this is valid only in the electrostatic limit $q \gg \omega/c$, which is the relevant regime for our case. Furthermore, since $n(\mathbf{q}) = \text{Tr}\{e^{-i\mathbf{q}\cdot\mathbf{r}}\rho\}$, one can write for the screening field,

$$V^s(\mathbf{q}) = V_c(q)4\sum_{n_1n_2\mathbf{k}}\langle n_1\mathbf{k}|e^{-i\mathbf{q}\cdot\mathbf{r}}|n_2\mathbf{k}+\mathbf{q}\rangle\langle n_2\mathbf{k}+\mathbf{q}|\rho|n_1\mathbf{k}\rangle, \tag{A7}$$

where we have taken into account two spin and two valley degeneracies. We are now interested in calculating the current response up to linear order in the external electric field $\mathbf{E}(t)$. Since the electric field is uniform in the graphene plane, we are only interested in the $\mathbf{q} = \mathbf{0}$ term, and the current density operator is given by $\mathbf{j}_{\text{op}} = -\frac{ev_F}{\Omega}\boldsymbol{\sigma}$. The induced current will have only the x component, since the electric field points in the x direction. Finally, the induced current density is given by $\mathbf{j} = \text{Tr}\{\mathbf{j}_{\text{op}}\,\rho\}$, so we can write

$$j_x = -\frac{ev_F}{\Omega}4\sum_{n_1n_2\mathbf{k}}\langle n_1\mathbf{k}|\sigma_x|n_2\mathbf{k}\rangle\langle n_2\mathbf{k}|\rho|n_1\mathbf{k}\rangle. \tag{A8}$$

To include also impurity scattering, we need to calculate the induced current up to second order in $V_i(\mathbf{q})$. In other words, we need to do a perturbation expansion of SPDM:

$$\rho = \rho_0 + \rho_l + \rho_i + \rho_{li} + \rho_{lii}, \tag{A9}$$

where ρ_0 is the equilibrium solution to Eq. (A1) for independent Dirac electrons in the absence of impurity scattering and light scattering, $\rho_l \propto H_l$ is the solution of Eq. (A1) correct up to linear order in light scattering, $\rho_i \propto H_i$ is the solution up to linear order in impurity scattering, $\rho_{li} \propto H_lH_i$ is the solution up to linear order in both light scattering and impurity scattering, and $\rho_{lii} \propto H_lH_i^2$ is the solution up to linear order in light scattering and quadratic in impurity scattering. Using Eq. (A1), we can now write the equation of motion for every order of SPDM expansion:

$$i\hbar\frac{\partial\rho_0}{\partial t} = [H_0,\rho_0], \tag{A10}$$

$$i\hbar\frac{\partial\rho_l}{\partial t} = [H_0,\rho_l] + \left[H_l + H_l^s,\rho_0\right], \tag{A11}$$

$$i\hbar\frac{\partial\rho_i}{\partial t} = [H_0,\rho_i] + \left[H_i + H_i^s,\rho_0\right], \tag{A12}$$

$$i\hbar\frac{\partial\rho_{li}}{\partial t} = [H_0,\rho_{li}] + \left[H_i + H_i^s,\rho_l\right] + \left[H_l + H_l^s,\rho_i\right] + \left[H_{li}^s,\rho_0\right], \tag{A13}$$

$$i\hbar\frac{\partial\rho_{lii}}{\partial t} = [H_0,\rho_{lii}] + \left[H_i + H_i^s,\rho_{li}\right] + \left[H_{li}^s,\rho_i\right] + \left[H_{lii}^s,\rho_0\right]. \tag{A14}$$

The equilibrium solution of Eq. (A10) describes the free electrons and is given by

$$\langle n_2\mathbf{k}+\mathbf{q}|\rho_0|n_1\mathbf{k}\rangle = \delta_{n_1,n_2}\delta_{\mathbf{q},0}f_{n_1\mathbf{k}}, \tag{A15}$$

where $\delta_{a,b}$ is the Kronecker delta symbol and $f_{n\mathbf{k}} = [e^{(E_{n\mathbf{k}}-E_F)/kT}+1]^{-1}$ is the Fermi-Dirac distribution at temperature T and Fermi energy E_F. Using relation (A15), we can write the solution of Eq. (A11) as

$$\langle n_2\mathbf{k}+\mathbf{q}|\rho_l|n_1\mathbf{k}\rangle = -i\frac{ev_F}{\omega}E_0\delta_{\mathbf{q},0}\langle n_2\mathbf{k}|\sigma_x|n_1\mathbf{k}\rangle\frac{f_{n_1\mathbf{k}}-f_{n_2\mathbf{k}}}{\hbar\omega+E_{n_1\mathbf{k}}-E_{n_2\mathbf{k}}}, \tag{A16}$$

which is a steady-state solution of SPDM that oscillates at frequency ω. Here we have used the following relation: $\langle n_2\mathbf{k}+\mathbf{q}|\sigma_x|n_1\mathbf{k}\rangle = \delta_{\mathbf{q},0}\langle n_2\mathbf{k}|\sigma_x|n_1\mathbf{k}\rangle$. We have neglected the screening field H_l^s in Eq. (A11) since the 2D electron gas cannot screen the uniform electric field. This can be seen below from Eq. (A40), which gives the dielectric function of graphene in the long-wavelength limit. One can immediately see that $\varepsilon(q=0,\omega)=1$, which means that there is no screening in the $q=0$ limit.

Let us now focus on Eq. (A12). We can introduce a self-consistent Hamiltonian $H_i^{\rm sc} = H_i + H_i^s$, and write $H_i^{\rm sc} = \frac{1}{\Omega}\sum_{\mathbf{q}}V_i^{\rm sc}(q)e^{i\mathbf{q}\cdot\mathbf{r}}$, where $V_i^{\rm sc} = V_i + V_i^s$ is a self-consistent scattering potential that consists of a bare impurity scattering potential V_i and a screening field V_i^s. By solving Eqs. (A7) and (A12) in a self-consistent way, one can show that $V_i^{\rm sc}(q) = V_i(q)/\varepsilon(q)$, where $\varepsilon(q)$ is the static dielectric function. The dynamic dielectric function of graphene is generally

$$\varepsilon(q,\omega) = 1 - V_c(q)\frac{4}{\Omega}\sum_{n_1n_2\mathbf{k}}\frac{f_{n_1\mathbf{k}}-f_{n_2\mathbf{k}+\mathbf{q}}}{\hbar\omega+E_{n_1\mathbf{k}}-E_{n_2\mathbf{k}+\mathbf{q}}} \times |\langle n_2\mathbf{k}+\mathbf{q}|e^{i\mathbf{q}\cdot\mathbf{r}}|n_1\mathbf{k}\rangle|^2, \tag{A17}$$

and one can simply check that $\varepsilon(q) = \varepsilon(q,\omega=0)$. Finally, the solution to Eq. (A12) can be written as

$$\langle n_2\mathbf{k}+\mathbf{q}|\rho_i|n_1\mathbf{k}\rangle = \frac{1}{\Omega}\frac{V_i(q)}{\varepsilon(q)}\frac{f_{n_1\mathbf{k}}-f_{n_2\mathbf{k}+\mathbf{q}}}{E_{n_1\mathbf{k}}-E_{n_2\mathbf{k}+\mathbf{q}}} \times \langle n_2\mathbf{k}+\mathbf{q}|e^{i\mathbf{q}\cdot\mathbf{r}}|n_1\mathbf{k}\rangle. \tag{A18}$$

To solve the next order of perturbation theory ρ_{li}, we need to include the screening field described by the Hamiltonian $H_{li}^s = \frac{1}{\Omega}\sum_{\mathbf{q}}V_{li}^s(\mathbf{q})e^{i\mathbf{q}\cdot\mathbf{r}}e^{-i\omega t}$ + c.c.. One can then solve Eq. (A13) by using results (A15), (A16), and (A18) to obtain

$$\begin{aligned}\langle n_2\mathbf{k}+\mathbf{q}|\rho_{li}|n_1\mathbf{k}\rangle = {}& \frac{1}{\Omega}V_{li}^s(\mathbf{q})\frac{f_{n_1\mathbf{k}}-f_{n_2\mathbf{k}+\mathbf{q}}}{\hbar\omega+E_{n_1\mathbf{k}}-E_{n_2\mathbf{k}+\mathbf{q}}}\langle n_2\mathbf{k}+\mathbf{q}|e^{i\mathbf{q}\cdot\mathbf{r}}|n_1\mathbf{k}\rangle + \frac{1}{\Omega}\frac{V_i(q)}{\varepsilon(q)}(-i)\frac{ev_F}{\omega}E_0\frac{1}{\hbar\omega+E_{n_1\mathbf{k}}-E_{n_2\mathbf{k}+\mathbf{q}}}\\ &\times\left(\sum_{n_3}\langle n_2\mathbf{k}+\mathbf{q}|e^{i\mathbf{q}\cdot\mathbf{r}}|n_3\mathbf{k}\rangle\langle n_3\mathbf{k}|\sigma_x|n_1\mathbf{k}\rangle\frac{f_{n_1\mathbf{k}}-f_{n_3\mathbf{k}}}{\hbar\omega+E_{n_1\mathbf{k}}-E_{n_3\mathbf{k}}} - \sum_{n_3}\langle n_2\mathbf{k}+\mathbf{q}|\sigma_x|n_3\mathbf{k}+\mathbf{q}\rangle\right.\\ &\times\langle n_3\mathbf{k}+\mathbf{q}|e^{i\mathbf{q}\cdot\mathbf{r}}|n_1\mathbf{k}\rangle\frac{f_{n_3\mathbf{k}+\mathbf{q}}-f_{n_2\mathbf{k}+\mathbf{q}}}{\hbar\omega+E_{n_3\mathbf{k}+\mathbf{q}}-E_{n_2\mathbf{k}+\mathbf{q}}} + \sum_{n_3}\langle n_2\mathbf{k}+\mathbf{q}|\sigma_x|n_3\mathbf{k}+\mathbf{q}\rangle\langle n_3\mathbf{k}+\mathbf{q}|e^{i\mathbf{q}\cdot\mathbf{r}}|n_1\mathbf{k}\rangle\\ &\left.\times\frac{f_{n_1\mathbf{k}}-f_{n_3\mathbf{k}+\mathbf{q}}}{E_{n_1\mathbf{k}}-E_{n_3\mathbf{k}+\mathbf{q}}} - \sum_{n_3}\langle n_2\mathbf{k}+\mathbf{q}|e^{i\mathbf{q}\cdot\mathbf{r}}|n_3\mathbf{k}\rangle\langle n_3\mathbf{k}|\sigma_x|n_1\mathbf{k}\rangle\frac{f_{n_3\mathbf{k}}-f_{n_2\mathbf{k}+\mathbf{q}}}{E_{n_3\mathbf{k}}-E_{n_2\mathbf{k}+\mathbf{q}}}\right).\end{aligned} \tag{A19}$$

Next, one can use relation (A7) to obtain the screening field in a self-consistent way:

$$\begin{aligned}V_{li}^s(\mathbf{q}) = {}& \frac{V_i(q)}{\varepsilon(q)}\frac{V_c(q)}{\varepsilon(q,\omega)}(-i)\frac{ev_F}{\omega}E_0\frac{4}{\Omega}\sum_{n_1n_2n_3\mathbf{k}}\frac{\langle n_1\mathbf{k}|e^{-i\mathbf{q}\cdot\mathbf{r}}|n_2\mathbf{k}+\mathbf{q}\rangle}{\hbar\omega+E_{n_1\mathbf{k}}-E_{n_2\mathbf{k}+\mathbf{q}}}\left(\langle n_2\mathbf{k}+\mathbf{q}|\sigma_x|n_3\mathbf{k}+\mathbf{q}\rangle\langle n_3\mathbf{k}+\mathbf{q}|e^{i\mathbf{q}\cdot\mathbf{r}}|n_1\mathbf{k}\rangle\right.\\ &\left.\times\frac{f_{n_1\mathbf{k}}-f_{n_3\mathbf{k}+\mathbf{q}}}{E_{n_1\mathbf{k}}-E_{n_3\mathbf{k}+\mathbf{q}}} - \langle n_2\mathbf{k}+\mathbf{q}|e^{i\mathbf{q}\cdot\mathbf{r}}|n_3\mathbf{k}\rangle\langle n_3\mathbf{k}|\sigma_x|n_1\mathbf{k}\rangle\frac{f_{n_3\mathbf{k}}-f_{n_2\mathbf{k}+\mathbf{q}}}{E_{n_3\mathbf{k}}-E_{n_2\mathbf{k}+\mathbf{q}}}\right),\end{aligned} \tag{A20}$$

where $\varepsilon(q,\omega)$ is the dynamic dielectric function given in (A17). Note that the terms containing $f_{n_1\mathbf{k}}-f_{n_3\mathbf{k}}$ and $f_{n_3\mathbf{k}+\mathbf{q}}-f_{n_2\mathbf{k}+\mathbf{q}}$ have disappeared after summation over n_1,n_2,n_3 and $\mathbf{k}$. One can also demonstrate the following important property: $V_{li}^s(-\mathbf{q}) = -V_{li}^s(\mathbf{q})$. Finally, one can use Eq. (A14) to find ρ_{lii}, and Eq. (A8) to find the induced current up to first order in light scattering and second order in impurity scattering:

$$\begin{aligned}j_x^{lii} = {}& -\frac{ev_F}{\Omega}4\sum_{n_1n_2n_3\mathbf{k},\mathbf{q}}\frac{\langle n_1\mathbf{k}|\sigma_x|n_2\mathbf{k}\rangle}{\hbar\omega+E_{n_1\mathbf{k}}-E_{n_2\mathbf{k}}}\left(\frac{1}{\Omega}\frac{V_i(q)}{\varepsilon(q)}\langle n_2\mathbf{k}|e^{-i\mathbf{q}\cdot\mathbf{r}}|n_3\mathbf{k}+\mathbf{q}\rangle\langle n_3\mathbf{k}+\mathbf{q}|\rho_{li}|n_1\mathbf{k}\rangle\right.\\ &-\frac{1}{\Omega}\frac{V_i(q)}{\varepsilon(q)}\langle n_2\mathbf{k}|\rho_{li}|n_3\mathbf{k}-\mathbf{q}\rangle\langle n_3\mathbf{k}-\mathbf{q}|e^{-i\mathbf{q}\cdot\mathbf{r}}|n_1\mathbf{k}\rangle + \frac{1}{\Omega}V_{li}^s(-\mathbf{q})\langle n_2\mathbf{k}|e^{-i\mathbf{q}\cdot\mathbf{r}}|n_3\mathbf{k}+\mathbf{q}\rangle\\ &\left.\times\langle n_3\mathbf{k}+\mathbf{q}|\rho_i|n_1\mathbf{k}\rangle - \frac{1}{\Omega}V_{li}^s(-\mathbf{q})\langle n_2\mathbf{k}|\rho_i|n_3\mathbf{k}-\mathbf{q}\rangle\langle n_3\mathbf{k}-\mathbf{q}|e^{-i\mathbf{q}\cdot\mathbf{r}}|n_1\mathbf{k}\rangle\right).\end{aligned} \tag{A21}$$

Note that we have neglected the screening field H^s_{lii} since we need only the $q = 0$ component of ρ_{lii} to obtain j_x^{lii}, and there is no screening in the 2D electron gas in the $q = 0$ case. Also note that we have skipped the lower orders in the induced current since one can generally show that $j_x^{li} = 0$. On the other hand, $j_x^l \neq 0$, but we are interested here in the optical absorption below the interband threshold $\hbar\omega < 2E_F$, where $\mathrm{Re}\, j_x^l = 0$. Finally, to evaluate the current component j_x^{lii} from expression (A21), we need to use expression (A18) for ρ_i and expression (A19) for ρ_{li}. The resulting conductivity is

$$\sigma_{lii}(\omega) = i\frac{e^2v_F^2}{\omega}\frac{1}{\Omega}\sum_{\mathbf{q}}\frac{1}{\Omega}\left|\frac{V_i(q)}{\varepsilon(q)}\right|^2\left(\frac{V_c(q)}{\varepsilon(q,\omega)}F^2(\mathbf{q},\omega)+\frac{4}{\Omega}\sum_{n_1n_2n_3n_4\mathbf{k}}G(n_1,n_2,n_3,\mathbf{k},\mathbf{q},\omega)\cdot H(n_1,n_2,n_4,\mathbf{k},\mathbf{q},\omega)\right), \tag{A22}$$

where the functions F, G, and H are given by the following expressions:

$$F(\mathbf{q},\omega) = -\frac{4}{\Omega}\sum_{n_1n_2n_3\mathbf{k}}\frac{f_{n_1\mathbf{k}}-f_{n_2\mathbf{k}+\mathbf{q}}}{E_{n_1\mathbf{k}}-E_{n_2\mathbf{k}+\mathbf{q}}}\left(\frac{\langle n_3\mathbf{k}|e^{-i\mathbf{q}\cdot\mathbf{r}}|n_2\mathbf{k}+\mathbf{q}\rangle}{\hbar\omega+E_{n_3\mathbf{k}}-E_{n_2\mathbf{k}+\mathbf{q}}}\langle n_2\mathbf{k}+\mathbf{q}|e^{i\mathbf{q}\cdot\mathbf{r}}|n_1\mathbf{k}\rangle\langle n_1\mathbf{k}|\sigma_x|n_3\mathbf{k}\rangle\right.$$
$$\left.-\langle n_1\mathbf{k}|e^{-i\mathbf{q}\cdot\mathbf{r}}|n_2\mathbf{k}+\mathbf{q}\rangle\frac{\langle n_2\mathbf{k}+\mathbf{q}|e^{i\mathbf{q}\cdot\mathbf{r}}|n_3\mathbf{k}\rangle}{-\hbar\omega+E_{n_3\mathbf{k}}-E_{n_2\mathbf{k}+\mathbf{q}}}\langle n_3\mathbf{k}|\sigma_x|n_1\mathbf{k}\rangle\right), \tag{A23}$$

$$G(n_1,n_2,n_3,\mathbf{k},\mathbf{q},\omega) = \frac{1}{\hbar\omega+E_{n_1\mathbf{k}}-E_{n_2\mathbf{k}+\mathbf{q}}}\left(\langle n_3\mathbf{k}|e^{-i\mathbf{q}\cdot\mathbf{r}}|n_2\mathbf{k}+\mathbf{q}\rangle\frac{\langle n_1\mathbf{k}|\sigma_x|n_3\mathbf{k}\rangle}{\hbar\omega+E_{n_1\mathbf{k}}-E_{n_3\mathbf{k}}}\right.$$
$$\left.-\langle n_1\mathbf{k}|e^{-i\mathbf{q}\cdot\mathbf{r}}|n_3\mathbf{k}+\mathbf{q}\rangle\frac{\langle n_3\mathbf{k}+\mathbf{q}|\sigma_x|n_2\mathbf{k}+\mathbf{q}\rangle}{\hbar\omega+E_{n_3\mathbf{k}+\mathbf{q}}-E_{n_2\mathbf{k}+\mathbf{q}}}\right), \tag{A24}$$

$$H(n_1,n_2,n_4,\mathbf{k},\mathbf{q},\omega) = \langle n_2\mathbf{k}+\mathbf{q}|e^{i\mathbf{q}\cdot\mathbf{r}}|n_4\mathbf{k}\rangle\langle n_4\mathbf{k}|\sigma_x|n_1\mathbf{k}\rangle\left(\frac{f_{n_1\mathbf{k}}-f_{n_4\mathbf{k}}}{\hbar\omega+E_{n_1\mathbf{k}}-E_{n_4\mathbf{k}}}-\frac{f_{n_4\mathbf{k}}-f_{n_2\mathbf{k}+\mathbf{q}}}{E_{n_4\mathbf{k}}-E_{n_2\mathbf{k}+\mathbf{q}}}\right)$$
$$+\langle n_2\mathbf{k}+\mathbf{q}|\sigma_x|n_4\mathbf{k}+\mathbf{q}\rangle\langle n_4\mathbf{k}+\mathbf{q}|e^{i\mathbf{q}\cdot\mathbf{r}}|n_1\mathbf{k}\rangle\left(-\frac{f_{n_4\mathbf{k}+\mathbf{q}}-f_{n_2\mathbf{k}+\mathbf{q}}}{\hbar\omega+E_{n_4\mathbf{k}+\mathbf{q}}-E_{n_2\mathbf{k}+\mathbf{q}}}+\frac{f_{n_1\mathbf{k}}-f_{n_4\mathbf{k}+\mathbf{q}}}{E_{n_1\mathbf{k}}-E_{n_4\mathbf{k}+\mathbf{q}}}\right). \tag{A25}$$

However, if we are interested only in the contribution from the collective excitations, we can neglect the single-particle excitations to obtain

$$\mathrm{Re}\sigma(\omega) = -\frac{e^2v_F^2}{\omega}\frac{1}{\Omega}\sum_{\mathbf{q}}\frac{1}{\Omega}\left|\frac{V_i(q)}{\varepsilon(q)}\right|^2F^2(\mathbf{q},\omega)V_c(q)\mathrm{Im}\frac{1}{\varepsilon(q,\omega)}. \tag{A26}$$

Note that this is the complete expression for the real part of the conductivity, i.e., $\mathrm{Re}\sigma(\omega) = \mathrm{Re}\sigma_{lii}(\omega)$, since $\mathrm{Re}\sigma_l(\omega) = 0$ in this regime, and generally $\mathrm{Re}\sigma_{li}(\omega) = 0$. Then, since we are only interested in the plasmon contribution, one can write the loss function as

$$\mathrm{Im}\frac{1}{\varepsilon(q,\omega)} = \frac{-\pi}{\frac{\partial\varepsilon}{\partial\omega}}\delta(\omega-\omega_q) = \frac{\pi}{\frac{\partial\varepsilon}{\partial q}}\delta(q-q_\omega), \tag{A27}$$

where ω_q is the plasmon frequency at a given wave vector q, and q_ω is the plasmon wave vector at a given frequency ω, which is determined by the zero of the dielectric function: $\varepsilon(q,\omega_q) = \varepsilon(q_\omega,\omega) = 0$. Note that δ function from Eq. (A27) extracts only a single wave vector from the integral $\int dq$ in Eq. (A26). Moreover, one can explicitly perform the remaining integral $\int d\varphi_{\mathbf{q}}$. To demonstrate this, we start by writing the expression for the Dirac wave function in coordinate representation:

$$\psi_{n,\mathbf{k}}(\mathbf{r}) = \langle\mathbf{r}|n\mathbf{k}\rangle = \frac{1}{\sqrt{2\Omega}}\begin{pmatrix} n \\ e^{i\varphi_{\mathbf{k}}}\end{pmatrix}e^{i\mathbf{k}\cdot\mathbf{r}}. \tag{A28}$$

It is straightforward to calculate the following matrix elements:

$$\langle n\mathbf{k}|e^{-i\mathbf{q}\cdot\mathbf{r}}|n'\mathbf{k}+\mathbf{q}\rangle = \tfrac{1}{2}(nn'+e^{-i\varphi_{\mathbf{k}}+i\varphi_{\mathbf{k}+\mathbf{q}}}), \tag{A29}$$

$$\langle n'\mathbf{k}+\mathbf{q}|e^{i\mathbf{q}\cdot\mathbf{r}}|n\mathbf{k}\rangle = \tfrac{1}{2}(nn'+e^{i\varphi_{\mathbf{k}}-i\varphi_{\mathbf{k}+\mathbf{q}}}), \tag{A30}$$

$$\langle n'\mathbf{k}|\sigma_x|n\mathbf{k}\rangle = \tfrac{1}{2}(ne^{-i\varphi_{\mathbf{k}}}+n'e^{i\varphi_{\mathbf{k}}}). \tag{A31}$$

Furthermore, the product of the last three terms can be written as

$$\langle n\mathbf{k}|e^{-i\mathbf{q}\cdot\mathbf{r}}|n'\mathbf{k}+\mathbf{q}\rangle\langle n'\mathbf{k}+\mathbf{q}|e^{i\mathbf{q}\cdot\mathbf{r}}|n''\mathbf{k}\rangle\langle n''\mathbf{k}|\sigma_x|n\mathbf{k}\rangle$$
$$=\left(\frac{1}{4}(1+nn'')+\frac{n'}{4}(n+n'')\frac{k+q\cos\varphi}{|\mathbf{k}+\mathbf{q}|}\right.$$
$$\left.+i\frac{n'}{4}(n-n'')\frac{q\sin\varphi}{|\mathbf{k}+\mathbf{q}|}\right)$$
$$\times\left(\frac{\cos\varphi}{2}[n''e^{i\varphi_{\mathbf{q}}}+ne^{-i\varphi_{\mathbf{q}}}]\right.$$
$$\left.+i\frac{\sin\varphi}{2}[n''e^{i\varphi_{\mathbf{q}}}-ne^{-i\varphi_{\mathbf{q}}}]\right), \tag{A32}$$

where $\varphi = \varphi_{\mathbf{k}} - \varphi_{\mathbf{q}}$. Finally, one can show that

$$F(\mathbf{q},\omega) = \tilde{F}(q,\omega)\cos\varphi_{\mathbf{q}}, \tag{A33}$$

where $\tilde{F}(q,\omega)$ depends only on the magnitude of the wave vector q and is given by the following expression:

$$\tilde{F}(q,\omega) = -\frac{4}{\Omega}\sum_{n_1n_2n_3\mathbf{k}} \frac{f_{n_1\mathbf{k}} - f_{n_2\mathbf{k}+\mathbf{q}}}{E_{n_1\mathbf{k}} - E_{n_2\mathbf{k}+\mathbf{q}}}\left(\frac{1}{\hbar\omega + E_{n_3\mathbf{k}} - E_{n_2\mathbf{k}+\mathbf{q}}} - \frac{1}{-\hbar\omega + E_{n_3\mathbf{k}} - E_{n_2\mathbf{k}+\mathbf{q}}}\right) \times \left\{ n_1(n_1+n_3)\left(n_1 + n_2\frac{k+q\cos\varphi}{|\mathbf{k}+\mathbf{q}|}\right)\frac{\cos\varphi}{4} + n_1(n_1-n_3)n_2\frac{q\sin\varphi}{|\mathbf{k}+\mathbf{q}|}\frac{\sin\varphi}{4}\right\}. \quad \text{(A34)}$$

Now one can indeed see that the integration over $d\varphi_{\mathbf{q}}$ in Eq. (A26) simply contributes with the following factor: $\int_0^{2\pi} d\varphi_{\mathbf{q}} \cos^2\varphi_{\mathbf{q}} = \pi$. Finally, Eq. (A26) is reduced to the following expression:

$$\mathrm{Re}\sigma(\omega) = -\frac{e^2v_F^2}{\omega}\frac{1}{4\pi}q\frac{1}{\Omega}\left|\frac{V_i(q)}{\varepsilon(q)}\right|^2 \tilde{F}^2(q,\omega)V_c(q)\left.\frac{\pi}{\frac{\partial\varepsilon(q,\omega)}{\partial q}}\right|_{\mathrm{pl}}, \quad \text{(A35)}$$

where q is the plasmon wave vector at the frequency ω. To evaluate this expression, one needs to calculate the double integral $\int dk \int d\varphi_{\mathbf{k}}$ to evaluate the function $\tilde{F}(q,\omega)$. This can be further simplified at zero temperature when the Fermi-Dirac distribution is a step function. In that case, we can group (n_1,n_2,n_3) and $(-n_1,-n_2,-n_3)$ terms in Eq. (A34) to obtain

$$\tilde{F}(q,\omega) = -\frac{2}{\Omega}\sum_{n_1n_2n_3\mathbf{k}} \frac{f_{\mathbf{k}} - f_{\mathbf{k}+\mathbf{q}}}{E_{n_1\mathbf{k}} - E_{n_2\mathbf{k}+\mathbf{q}}}\left(\frac{1}{\hbar\omega + E_{n_3\mathbf{k}} - E_{n_2\mathbf{k}+\mathbf{q}}} - \frac{1}{-\hbar\omega + E_{n_3\mathbf{k}} - E_{n_2\mathbf{k}+\mathbf{q}}}\right) \times \left\{ n_1(n_1+n_3)\left(n_1 + n_2\frac{k+q\cos\varphi}{|\mathbf{k}+\mathbf{q}|}\right)\frac{\cos\varphi}{4} + n_1(n_1-n_3)n_2\frac{q\sin\varphi}{|\mathbf{k}+\mathbf{q}|}\frac{\sin\varphi}{4}\right\}, \quad \text{(A36)}$$

where $f_{\mathbf{k}} = f_{n=1,\mathbf{k}}$ stands for the Fermi-Dirac distribution of the conduction band, and we have assumed electron doping, i.e., $E_F > 0$. We perform a numerical integration to evaluate the function $\tilde{F}(q,\omega)$; however, one can obtain a closed expression in the small frequency limit when $\hbar\omega \ll E_F$. In that case, only intraband transitions contribute and one can set $n_1 = n_2 = n_3 = 1$ in Eq. (A36). Furthermore, in that case the plasmon wave vector q is much smaller than the Fermi wave vector q_F, so one can use the long-wavelength expansions

$$E_{\mathbf{k}} - E_{\mathbf{k}+\mathbf{q}} = -\nabla_{\mathbf{k}}E_{\mathbf{k}}\cdot\mathbf{q}, \quad \text{(A37)}$$

$$f_{\mathbf{k}} - f_{\mathbf{k}+\mathbf{q}} = -\frac{\partial f}{\partial E}(\nabla_{\mathbf{k}}E_{\mathbf{k}}\cdot\mathbf{q}). \quad \text{(A38)}$$

Next, it is straightforward to perform integration in Eq. (A36) to obtain the long-wavelength (small frequency) approximation:

$$\tilde{F}(q,\omega) = -\frac{q}{\pi\hbar^2\omega v_F}. \quad \text{(A39)}$$

In a similar manner, from Eq. (A17), one can obtain the dielectric function in this approximation:

$$\varepsilon(q,\omega) = 1 - \frac{q}{\omega^2}\frac{e^2v_F\sqrt{n}}{2\bar{\varepsilon}_r\varepsilon_0\hbar\sqrt{\pi}}, \quad \text{(A40)}$$

which is just the Drude model for the dielectric function in graphene [3].

Finally, from Eq. (A35) we obtain optical absorption in the small frequency limit:

$$\mathrm{Re}\sigma(\omega) = \frac{\pi e^2}{4\hbar}\frac{n_i}{q_{\mathrm{TF}}^2}\left(\frac{\hbar\omega}{E_F}\right)^3, \quad \text{(A41)}$$

where $q_{\mathrm{TF}} = \frac{e^2q_F}{\pi\bar{\varepsilon}_r\varepsilon_0\hbar v_F}$ is the Thomas-Fermi wave vector.

[1] W. L. Barnes, A. Dereux, and T. W. Ebbesen, Nature (London) **424**, 824 (2003).
[2] P. R. West, S. Ishii, G. V. Naik, N. K. Emani, V. M. Shalaev, and A. Boltasseva, Laser Photon. Rev. **4**, 795 (2010).
[3] M. Jablan, H. Buljan, and M. Soljačić, Phys. Rev. B **80**, 245435 (2009).
[4] M. Jablan, M. Soljačić, and H. Buljan, Invited paper in Proc. IEEE **101**, 1689 (2013).
[5] K. S. Novoselov *et al.*, Science **306**, 666 (2004).
[6] K. S. Novoselov, D. Jiang, F. Schedin, T. J. Booth, V. V. Khotkevich, S. V. Morozov, and A. K. Geim, Proc. Natl. Acad. Sci. (U.S.A.) **102**, 10451 (2005).
[7] Z. Fei, A. S. Rodin, G. O. Andreev, W. Bao, A. S. McLeod, M. Wagner, L. M. Zhang, Z. Zhao, M. Thiemens, G. Dominguez, M. M. Fogler, A. H. Castro-Neto, C. N. Lau, F. Keilmann, and D. N. Basov, Nature (London) **487**, 82 (2012).
[8] H. Yan, T. Low, W. Zhu, Y. Wu, M. Freitag, X. Li, F. Guinea, P. Avouris, and F. Xia, Nat. Photon. **7**, 394 (2013).
[9] Z. Fang, S. Thongrattanasiri, A. Schlater, Z. Liu, L. Ma, Y. Wang, P. M. Ajayan, P. Nordlander, N. J. Halas, and F. J. Garcia de Abajo, ACS Nano **7**, 2388 (2013).
[10] Y. Liu, R. F. Willis, K. V. Emtsev, and Th. Seyller, Phys. Rev. B **78**, 201403(R) (2008).
[11] T. Nagao, T. Hildebrandt, M. Henzler, and S. Hasegawa, Phys. Rev. Lett. **86**, 5747 (2001).
[12] R. R. Nair, P. Blake, A. N. Grigorenko, K. S. Novoselov, T. J. Booth, T. Stauber, N. M. R. Peres, and A. K. Geim, Science **320**, 1308 (2008).
[13] Z. Q. Li, E. A. Henriksen, Z. Jiang, Z. Hao, M. C. Martin, P. Kim, H. L. Stormer, and D. N. Basov, Nat. Phys. **4**, 532 (2008).
[14] T. Stauber, N. M. R. Peres, and A. H. Castro Neto, Phys. Rev. B **78**, 085418 (2008).

[15] J. P. Carbotte, E. J. Nicol, and S. G. Sharapov, Phys. Rev. B **81**, 045419 (2010).
[16] N. M. R. Peres, R. M. Ribeiro, and A. H. Castro Neto, Phys. Rev. Lett. **105**, 055501 (2010).
[17] F. T. Vasko, V. V. Mitin, V. Ryzhii, and T. Otsuji, Phys. Rev. B **86**, 235424 (2012).
[18] B. Scharf, V. Perebeinos, J. Fabian, and P. Avouris, Phys. Rev. B **87**, 035414 (2013).
[19] E. H. Hwang, S. Adam, and S. Das Sarma, Phys. Rev. Lett. **98**, 186806 (2007).
[20] K. Kechedzhi and S. Das Sarma, Phys. Rev. B **88**, 085403 (2013).
[21] J. J. Hopfield, Phys. Rev. **139**, A419 (1965).
[22] G. D. Mahan, *Many-Particle Physics*, 3rd ed. (Kluwer Academic/Plenum, New York, 2000).
[23] D. Pines, *Elementary Excitations in Solids* (Perseus Books, Reading, Massachusetts, 1999).
[24] F. Stern, Phys. Rev. Lett. **18**, 546 (1967).
[25] E. H. Hwang and S. Das Sarma, Phys. Rev. B **75**, 205418 (2007).
[26] A. Konar, T. Fang, and D. Jena, Phys. Rev. B **82**, 115452 (2010).
[27] A. Ron, Phys. Rev. **131**, 2041 (1963).
[28] P. R. Wallace, Phys. Rev. **71**, 622 (1947).
[29] G. W. Semenoff, Phys. Rev. Lett. **53**, 2449 (1984).